Available online at www.eccomasproceedia.org
Eccomas Proceedia SMART (2023) 203-213

ECCOMAS
Proceedia

X ECCOMAS Thematic Conference on Smart Structures and Materials
SMART 2023
D.A. Saravanos, A. Benjeddou, N. Chrysochoidis and T. Theodosiou (Eds)

MULTIMODAL VIBRATION DAMPING OF A THIN CIRCULAR RING COUPLED TO AN ANALOGOUS PIEZOELECTRIC NETWORK: NUMERICAL ANALYSIS

ALAN LUO*, BORIS LOSSOUARN† AND ALPER ERTURK*

* Georgia Institute of Technology
771 Ferst Dr NW, Atlanta, Georgia 30313, United States
e-mail: luo@gatech.edu

† Conservatoire national des arts et métiers
HESAM Université
292 Rue Saint-Martin, 75003 Paris, France
e-mail: boris.lossouarn@lecnam.net

Key words: Multimodal Damping, Vibration Control, Broadband, Piezoelectric, Electrical Networks

Abstract. Vibrations in structures can be reduced by coupling to a piezoelectric electrical network that exhibits analogous modal properties of the structure. This paper considers the multimodal vibration damping of a thin circular ring using this method. The electrical network is derived by applying a finite difference model to the governing equations of motion for a segment of a thin curved beam and applying an electromechanical analogy to the physical constants. The resulting discrete network for a curved beam segment can be assembled into a complete network for a circular ring. The electrical network for a circular ring displays modal properties similar to its mechanical analogue in both the spatial and frequency domains. Numerical simulation demonstrates the effectiveness and robustness of the broadband damping effects from the analogous network.

1 INTRODUCTION

Analogous electrical networks of mechanical structures implemented with passive components were originally theorised and developed in the 1940s by MacNeal [1] for computational purposes of determining the structural responses in beams [2], plates [3], stiffened shells [4], and even entire aerospace structures [5]. Eventually, analogous electrical networks of mechanical structures were separately theorized and developed specifically for the purposes of vibration control, which had demonstrated the most optimal electromechanical coupling [6], [7]. These analogous networks were theorized for beams [8] as well as thin plates [9], [10], yet were never experimentally validated due to the complexity of the circuit architecture. Attempts of using synthetic components with operational amplifiers have been proposed in building the analogue of a beam [11], but as with active components, run into stability issues [12].

Peer-review under responsibility of the organizing committee of SMART 2023.
doi: 10.7712/150123.9778.444165

The electrical networks were redesigned and simplified [13], [14] by applying a finite difference scheme to the classical mechanical equations of motion, which reduced the number of components required to assemble. Further experimental validation using this method was confirmed for rods [15], beams [13], plates [14], and most recently curved beams [16]. The networks were tested through experimental modal analysis to observe the electrical structure-like mode shapes. As a result of the matching mode shapes between the electrical and mechanical domain, the network acts as a vibration absorber at every point on the structure rather than the discrete point absorber of a distributed piezoelectric transducer network. Coarse arrays of piezoelectric transducers, altered boundary conditions, and local defects were introduced to the structure, yet the analogous network still produced effective multimodal damping.

In this study, we extend the study of vibration damping by an analogous electrical network to thin circular rings. The electrical network is derived by applying a finite difference model to the governing equations of motion for a segment of a thin curved beam and applying an electromechanical analogy to the physical constants as well as the internal forces and moments. The resulting discrete network unit cell for a curved beam segment can be assembled into a complete network for a circular ring by forming a loop between the first and last unit cells. An inextensional neutral axis assumption is applied to the equations of motions of the curved beam network in order to simplify the topology of the electrical network. The electrical network for a circular ring displays modal properties similar to its mechanical analogue in both the spatial and frequency domain. By increasing the number of discrete unit cells in the network, it is theoretically possible to replicate the entire frequency spectrum of the ring in the electrical domain. The ring and the electrical network are coupled using piezoelectric patches, which act as capacitive elements in the network. Numerical simulations of a ring coupled to the analogous network using optimal dissipative components demonstrate the validity and effectiveness of the theory.

2 ELECTRICAL ANALOGUE OF A CURVED BEAM

2.1 Extensional equations of motion

The equations of motion for an extensional thin curved beam of density ρ, cross sectional area S, and radius of curvature R, is modelled using the same assumptions as the Euler-Bernoulli beam theory [17]. After summing the internal moments and forces of an infinitesimal segment of a curved beam, the governing equations of motions are given by:

$$\frac{\partial N}{\partial s} + \frac{Q}{R} = \rho S \frac{\partial^2 v}{\partial t^2}, \qquad \frac{\partial Q}{\partial s} - \frac{N}{R} = \rho S \frac{\partial^2 w}{\partial t^2}, \tag{1}$$

where N is the normal force in the beam and Q is the shear force in the beam. The term w is the displacement in the transverse direction, denoted by the coordinate z, and the term v is the displacement in the circumferential direction, denoted by the coordinate s. Following Euler-Bernoulli beam theory, the shear force can be related to the bending moment M. Shear deformations can also be treated as negligible, so the slope of the beam θ is directly related to the displacements. Furthermore, the normal force N and the bending moment M can also be related to the displacements. With all of these assumptions, the internal forces, moments, and kinematic relationships can be rewritten as first order state equations given by:

$$\begin{aligned} Q &= -\frac{\partial M}{\partial s}, & \theta &= \frac{\partial w}{\partial s} - \frac{v}{R}, \\ M &= EI\frac{\partial \theta}{\partial s}, & N &= ES\left(\frac{\partial v}{\partial s} + \frac{w}{R}\right). \end{aligned} \tag{2}$$

where E is the Young's modulus and I is the second moment of area.

2.2 Inextensional equations of motion and network simplifications

For in-plane vibrations of thin circular beams or rings, the theory of inextension can adequately determine properties of the structure vibrating at low frequencies, as derived by Lang [18]. The inextensional equations of a thin curved beam assume that the extension of the neutral axis of the ring is negligible compared to the bending deformation. The assumption relates the radial displacement and the tangential slope as $w = -R\frac{\partial v}{\partial s}$, which reduces the normal force N in 2 to 0, leaving the first order equations:

$$Q = -\frac{\partial M}{\partial s}, \qquad M = EI\frac{\partial \theta}{\partial s}, \qquad \theta = \frac{\partial w}{\partial s} - \frac{v}{R}. \tag{3}$$

Applying a finite difference scheme and an electromechanical analogy to the equations of motion [16], the discretized set of analogous electrical equations can be given as:

$$\begin{aligned} -\frac{L}{2}\omega^2 q_{v_L} &= V_{v_I} - V_{v_L} + \frac{\hat{a}}{2\hat{R}}V_{w_L}, & \frac{\hat{a}}{2}V_{w_L} &= V_{\theta_L} - V_{\theta_I}, \\ -\frac{L}{2}\omega^2 q_{v_R} &= V_{v_R} - V_{v_I} + \frac{\hat{a}}{2\hat{R}}V_{w_R}, & \frac{\hat{a}}{2}V_{w_R} &= V_{\theta_I} - V_{\theta_L}, \\ -L\omega^2 q_{w_I} &= V_{w_R} - V_{w_L} - \frac{\hat{a}}{\hat{R}}V_{v_I}, & \frac{\hat{a}}{2}q_{\theta_L} &= q_{w_I} - q_{w_L} - \frac{\hat{a}}{2\hat{R}}q_{v_L}, \\ C_\theta V_{w_I} &= q_{\theta_R} - q_{\theta_L}, & \frac{\hat{a}}{2}q_{\theta_R} &= q_{w_R} - q_{w_I} - \frac{\hat{a}}{2\hat{R}}q_{v_R}. \end{aligned} \tag{4}$$

where $\hat{a}$ refers to the length of the unit cell in the finite difference scheme. The inductance L is the electrical analogue of the mass of the unit cell, which replaces the mechanical term ρSa. Likewise, the capacitance C_θ is the electrical analogue of the stiffness in the unit cell, replacing the mechanical term a/EI.

The network may be further simplified by considering that when assembled, the edge transformers may be combined to form a single transformer with twice the transformer ratio [15]. Furthermore, the two $L/2$ inductors can be combined into a single L inductor. Although combining the inductors is not analytically equivalent, it is a good approximation with enough unit cells. The resulting simplified network is shown in Figure 1.

2.3 Spatial and frequency coherence

In order to ensure that the electrical modes correspond to the same mechanical modes, spatial and frequency conditions must be applied to determine the correct electrical constants.

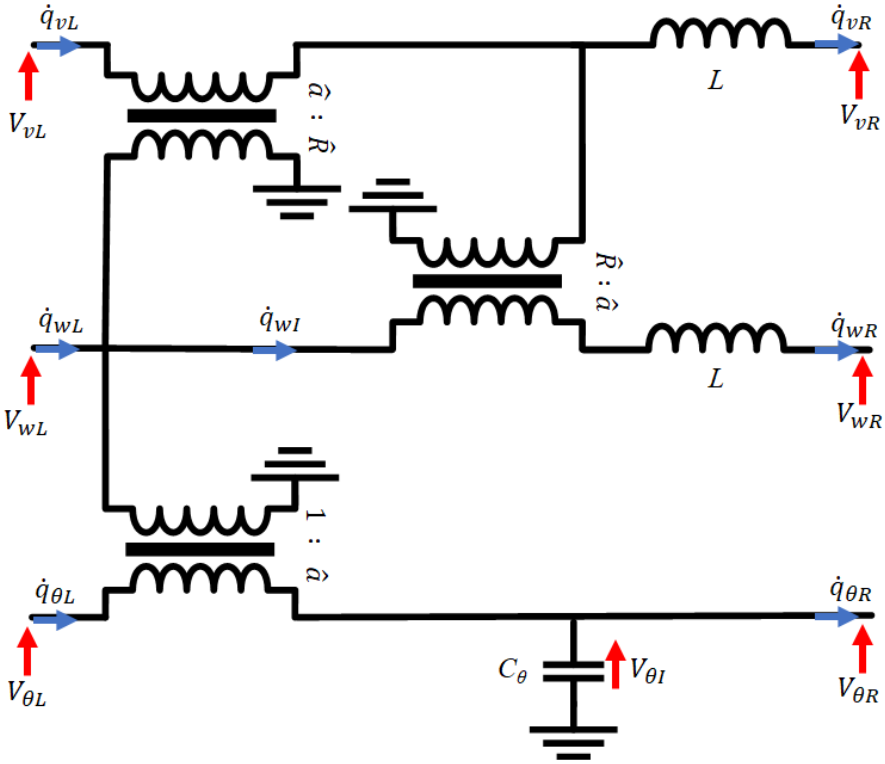

Figure 1: Simplified electrical unit cell.

Spatial coherence refers to the likeness of the physical shapes of the mechanical modes to the physical shapes of the electrical modes. This not only includes ensuring adequate discretization so that the desired mode shapes may be accurately represented, but also account for the correct mechanical boundary conditions in the electrical domain. Without enough unit cells of the electrical network, spatial modes may be aliased and not representative of the actual mode shape of the ring. Spatial coherence can be assured by adhering to the criteria previously described in [15] as

$$\frac{n_{element}}{N_{max}} \geq 10, \tag{5}$$

which says that the number of elements in the structure ($n_{element}$) has to be ten times or greater than the maximum number of wavelengths (N_{max}) in the frequency range.

Frequency coherence ensures that the natural frequencies for the electrical network matches the natural frequencies of the mechanical ring which means that the two domains have similar wave propagation properties. Although applying a strict electromechanical analogy between the two domains is a possibility of ensuring frequency coherence, it is not necessary or ideal as it constrains the degree of freedom in network tuning. Instead, the frequency coherence is derived by equating the mechanical and electrical transfer matrices as shown by Darleux [16]. For the frequency coherence of a curved beam element, the conditions are given as:

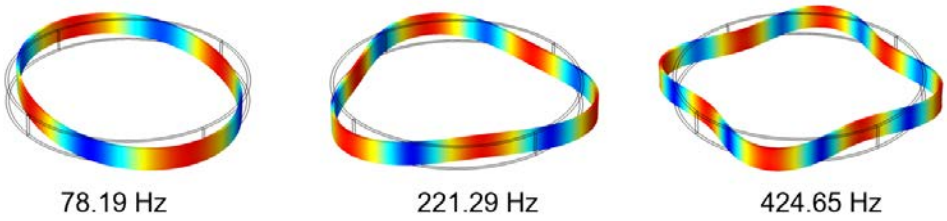

Figure 2: Mechanical bending mode shapes of a circular ring

$$\frac{a}{R} = \frac{\hat{a}}{\hat{R}}, \qquad \frac{K_\theta}{a^2 m} = \frac{1}{\hat{a}^2 L C_\theta}. \tag{6}$$

3 NUMERICAL ANALYSIS

3.1 Electrical network validation

The first 3 in-plane circumferential bending modes are simulated for an aluminum ring with free boundary conditions of radius $R = 200$ mm, width $b = 40$ mm, and thickness $h_s = 5$ mm. The ring is formed from a sheet of aluminum 6061 with Poisson's ratio of 0.33, Young's Modulus of 69 GPa, and density of 2700 kg/m^3. The circumferential mechanical bending modes are shown in Figure 2. Also note that for circular structures, there are pairs of mode at each frequency.

The simplified electrical network is tested using a unit cell count of $n = 100$. Since the electrical network is only representative of the circumferential bending equations, any out-of-plane twist-bending modes are not reflected in the electrical eigenvalues. For large number of unit cells, the convergence of the network is very close to the mechanical modes. The resulting eigenvalues are shown in Table 1. The electrical eigenvalues are within 2% of the corresponding mechanical eigenvalues. The correlation at higher modes drifts apart due to the finite difference approximation and finite number of unit cells. At higher unit cell counts, it is possible to improve the correlation at higher modes.

Table 1: Comparison of the natural frequencies of the electrical network to the mechanical natural frequencies for $n = 100$ unit cells. The percent difference between the two modes are shown in parentheses.

Mechanical Ring	**Electrical Simplified Network**
78.19 Hz	77.51 Hz (1.09%)
221.29 Hz	218.89 Hz (1.34%)
424.65 Hz	418.74 Hz (1.68%)

From the numerical simulations, it is possible to extract the electrical currents across each inductor on the w line to construct a spatial representation of the electrical mode shapes, as shown in Figure 3. Through the direct electromechanical analogy, the current through each inductor is equivalent to the transverse velocity of the ring at each discrete segment. Like the modes of the mechanical ring, each natural frequency has a pair of modes. Comparing the

spatial visualization of the electrical mode shapes to the circumferential mechanical bending modes shown in Figure 3, we can confirm good spatial and frequency coherence between the two domains.

Figure 3: Spatial visualization of the electrical mode shapes for a network of 100 unit cells.

To validate the network frequency response, an equivalent voltage excitation must be placed in the unit cell to simulate the mechanical excitation between unit cells in the ring. The equivalent voltage excitation should be placed on the transverse vibration voltage line, V_w. To avoid introducing an unwanted ground in the network direct voltage excitation is avoided. Instead, a 1:1 transformer is used as a buffer between the voltage source and the rest of the network in order to maintain the circuit topology and measure the correct frequency response.

In the electrical network, the measurement point is the voltage across the inductor of the unit cell where the excitation voltage is applied. This measurement is equivalent to the direct drive measurement in a mechanical structure, where the acceleration of the point is measured where the excitation force is applied. Figure 4 shows the voltage frequency response of the 21 unit cell electrical network with a direct drive measurement, where the voltage measurement is taken at the same point as the excitation point. Around the resonance frequencies, each spatial representation of the electrical current shows an operational mode shape that is similar to the corresponding mechanical mode shape.

3.2 Modeling and simulation of the coupled system

PI DuraAct Patch Transducers P-876.A15 are used to couple the electrical network to the ring. The piezoelectric material in this encapsulated patch is PIC255. The full dimension of the patch are 61 mm by 35 mm; however, the active material within the patch only measures 50 mm by 30 mm, as seen in Figure 5. Therefore, when modeling the patch, we consider the complete dimension of the patch in order to determine the theoretical maximum number of patches that will fit on the ring, but only the dimensions of the active material is actually used to model the patch in order to accurately account for the piezoelectric effect of the patch. The piezoelectric patches have a free capacitance of $C_\theta = 45$ nF.

Following the method used by Pernod [19], the encapsulated patch is modeled in two layers: the kapton-glue section and the PIC255 active section. By integrating the surface charge across a piezoelectric patch from a 1 V input voltage, it was observed that patch capacitance falls closer to 36 nF. Using this capacitance value, the other electrical constants such as the inductance and the transformer ratios are derived from the frequency coherence conditions. The values of the electrical components are shown in Table 2.

A theoretical maximum of 21 piezoelectric patches are attached to the exterior surface of a

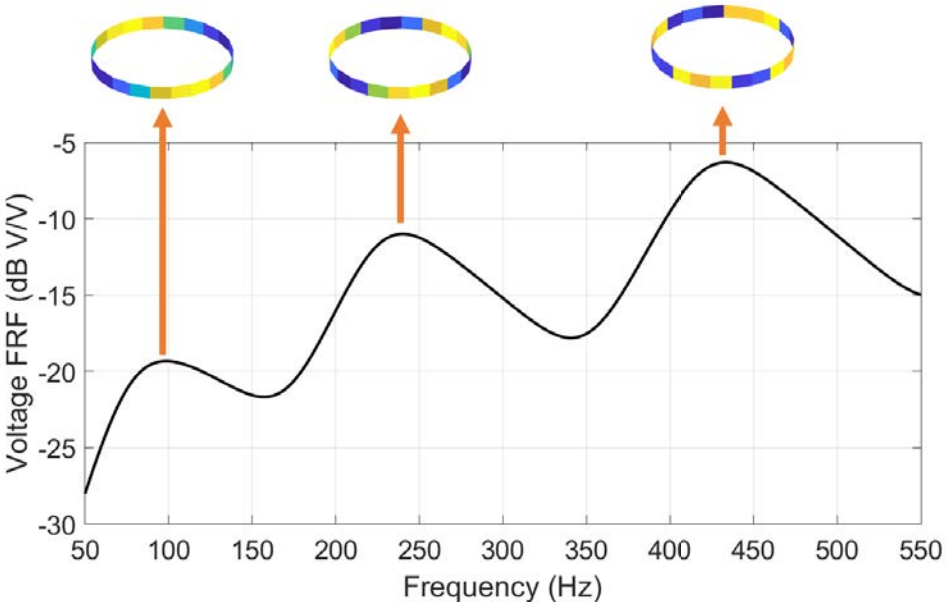

Figure 4: Numerical electrical frequency response function of a 21 unit cell network (—), with operational mode shapes shown for each corresponding mode.

Table 2: Values of components used in the electrical unit cell.

Electrical Component	**Value**
Capacitor (C_θ)	36 nF
Inductor (L)	418.7 mH
Transformer ($\hat{a} : \hat{R}$)	0.2992
Transformer ($\hat{a} : 1$)	4

200 mm radius ring in the COMSOL model. The model of the ring does not consider mechanical damping. The electromechanical coupling factor, the conversion rate between electrical energy and mechanical energy, of the piezoelectric patches is given by

$$k_C = \sqrt{\frac{\omega_{OC}^2 - \omega_{SC}^2}{\omega_{SC}^2}}, \tag{7}$$

where ω_{OC} is the open circuit frequency and ω_{SC} is the short circuit frequency of the piezoelectric ring. The electromechanical coupling factors of the ring for the first six circumferential bending modes are shown in 3. Note that each mode exists in pairs for circular structures, so for each mode of wavelength N, there are two separate coupling factors.

The frequency response is measured using a direct drive method, where the measurement point coincides with the frequency sweep excitation point, as shown in Figure 6. The measurement and excitation point is chosen to be directly on the neutral axis of the ring in order to avoid any excitation of the twisting modes of the structure, which cannot be controlled by this electrical network.

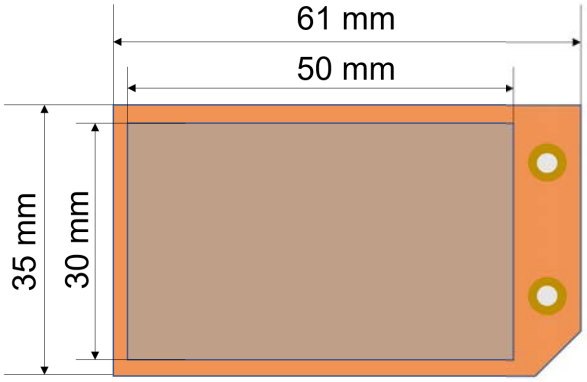

Figure 5: P0876.A15 patch dimensions.

Table 3: Electromechanical coupling factors for the first six modes of a circular ring.

Mode	**Coupling Factors**, k_C
N=2	12.73% and 13.04%
N=3	12.80% and 13.09%
N=4	12.82% and 13.15%

A frequency response function is shown for the coupled system in Figure 7. The first three resonances are shown in the considered frequency range of the plot. For comparison, the open circuit response is shown together with the coupled responses.

Resistors can be placed in series with the 1:4 transformer as dissipative components according to Lossouarn [20] following

$$R_T \approx 0.6 k_C \hat{a} \sqrt{2L/C} \tag{8}$$

where k_C is the coupling factor. This dissipative model is computed and a significant vibration damping can be observed.

For a 21 unit cell network, according to the spatial coherence wavelength criteria in Equation 5, only the first pair ring mode, with 2 wavelengths, can be ideally tuned. For a well tuned mode, the two local maxima on the frequency response function should have approximately the same amplitude, which is observed for the first mode ($N = 2$). At the next two higher modes ($N = 3, 4$), this is not observed, indicating that a 21 unit cells network is not enough to perfectly optimize the second and third mode, which have three and four wavelengths, respectively. Following the spatial coherence wavelength criteria previously discussed in Equation 5, the electrical network should have a minimum of 40 unit cells in order to ensure that all three electromechanical mode pairs have equal amplitudes. Nevertheless, using a 21 unit cell network, which considers the real dimensions of piezoelectric patches, still demonstrates strong coupling and vibration attenuation.

4 CONCLUSION

This study investigated the multimodal damping of a piezoelectric circular ring connected to an analogous electrical network. The analogous network was designed to exhibit the same

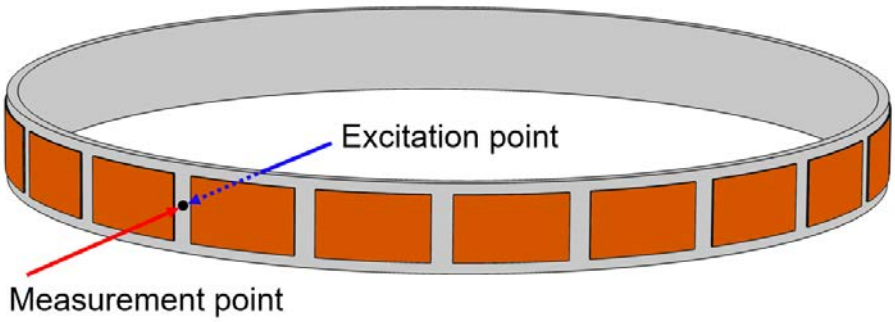

Figure 6: COMSOL model of the ring with 21 piezoelectric patches. The drive point measurement to obtain the frequency response is indicated on the figure.

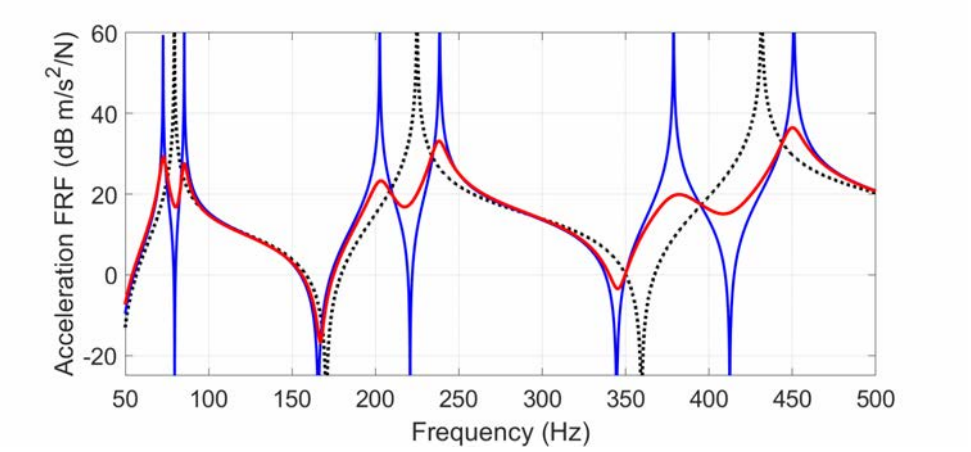

Figure 7: Frequency response functions of the ring coupled to its analogous network in open circuit (·····), with a non-dissipative electrical network (——), and with a dissipative electrical network (——)

modal properties as a mechanical ring structure. The previously derived network for a curved beam was simplified using the inextensional assumption of the neutral axis of the ring. Further simplifications involved combining adjacent transformers and inductors, effectively reducing the number of components in the electrical network. Spatial and frequency coherence was verified, which validated the analogy between the ring and the electrical network.

Numerical simulation were conducted using practical considerations, such as modeling encapsulated piezoelectric patches bonded to the curvature of the ring and optimal network resistance based on coupling factors. Significant vibration attenuation was observed when the ring was coupled to an optimally dissipative network, with optimal tuning observed for the first mode. Less optimal tuning occurred for the second and third modes due to the insufficient unit cells along the circumference of the ring, but vibration attenuation was still significant. Further experimental testing on the ring will be performed to verify the robustness and tunability of the broadband damping effects from the analogous network.

5 ACKNOWLEDGEMENTS

This research was funded in part by the Chateaubriand Fellowship awarded by the Embassy of France in the United States. The fellowship opened up opportunities for collaboration and professional development.

References

[1] R. H. MacNeal, "The solution of partial differential equations by means of electrical networks. dissertation (ph.d.)," Thesis, 1949.

[2] S. U. Benscoter and R. H. MacNeal, "Introduction to electrical-circuit analogies for beam analysis," Thesis, 1952.

[3] S. U. Benscoter and R. H. MacNeal, "Equivalent-plate theory for a straight multicell wing," Thesis, 1952.

[4] R. H. MacNeal, "Electrical analogies for stiffened shells with exible rings," NACA, Report, 1954.

[5] R. MacNeal, *Electric Circuit Analogies for Elastic Structures* (Airplane, missle and spacecraft structure series). John Wiley & Sons Canada, Limited, 1962, ISBN: 9780471560494. [Online]. Available: https://books.google.com/books?id=RNC7zQEACAAJ.

[6] S. Alessandroni, F. dell'Isola, and M. Porfiri, "A revival of electric analogs for vibrating mechanical systems aimed to their efficient control by pzt actuators," *International Journal of Solids and Structures*, vol. 39, no. 20, pp. 5295–5324, 2002, ISSN: 0020-7683. DOI: https://doi.org/10.1016/S0020-7683(02)00402-X. [Online]. Available: https://www.sciencedirect.com/science/article/pii/S002076830200402X.

[7] F. dell'Isola, M. Porfiri, and S. Vidoli, "Piezo-electromechanical (PEM) structures: Passive vibration control using distributed piezoelectric transducers," *Comptes Rendus Mécanique*, vol. 331, no. 1, pp. 69–76, 2003, ISSN: 1631-0721. DOI: https://doi.org/10.1016/S1631-0721(03)00022-6. [Online]. Available: https://www.sciencedirect.com/science/article/pii/S1631072103000226.

[8] M. Porfiri, F. dell'Isola, and F. M. Frattale Mascioli, "Circuit analog of a beam and its application to multimodal vibration damping, using piezoelectric transducers," *International Journal of Circuit Theory and Applications*, vol. 32, no. 4, pp. 167–198, 2004, ISSN: 0098-9886. DOI: https://doi.org/10.1002/cta.273. [Online]. Available: https://doi.org/10.1002/cta.273.

[9] S. Alessandroni, U. Andreaus, F. dell'Isola, and M. Porfiri, "A passive electric controller for multimodal vibrations of thin plates," *Computers & Structures*, vol. 83, no. 15, pp. 1236–1250, 2005, ISSN: 0045-7949. DOI: https://doi.org/10.1016/j.compstruc.2004.08.028. [Online]. Available: http://www.sciencedirect.com/science/article/pii/S0045794905000283.

[10] S. Alessandroni, U. Andreaus, F. dell Isola, and M. Porfiri, "Piezo-electromechanical (PEM) kirchho-love plates," *European Journal of Mechanics - A/solids*, vol. 23, no. 4, pp. 689–702, 2004.

[11] M. Panella, M. Paschero, and F. F. Mascioli, "Optimised RC-active synthesis of PEM networks," English, *Electronics Letters*, vol. 41, 1041–1043(2), 19 Sep. 2005, ISSN: 0013-

5194. [Online]. Available: https://digital-library.theiet.org/content/journals/10.1049/el_20051847.

[12] M. Panella, M. Paschero, and F. F. Mascioli, "Stability analysis of optimal PEM networks," English, *Electronics Letters*, vol. 42, 961–963(2), 17 Aug. 2006, ISSN: 0013-5194. [Online]. Available: https://digital-library.theiet.org/content/journals/10.1049/el_20062114.

[13] B. Lossouarn, M. Aucejo, J. F. Deu, and K. A. Cunefare, "Design of a passive electrical analogue for piezoelectric damping of a plate," *Journal of Intelligent Material Systems and Structures*, vol. 29, no. 7, pp. 1301–1314, 2018, ISSN: 1045-389x. DOI: 10.1177/1045389x17731232. [Online]. Available: %3CGo%20to%20ISI%3E://WOS:000432088000003.

[14] B. Lossouarn, J. F. Deu, and M. Aucejo, "Multimodal vibration damping of a beam with a periodic array of piezoelectric patches connected to a passive electrical network," *Smart Materials and Structures*, vol. 24, no. 11, 2015, ISSN: 0964-1726. DOI: Artn11503710.1088/0964-1726/24/11/115037. [Online]. Available: %3CGo%20to%20ISI%3E://WOS:000366111400039.

[15] B. Lossouarn, M. Aucejo, and J. F. Deü, "Multimodal coupling of periodic lattices and application to rod vibration damping with a piezoelectric network," *Smart Materials and Structures*, vol. 24, no. 4, p. 045 018, Feb. 2015. DOI: 10.1088/0964-1726/24/4/045018. [Online]. Available: https://doi.org/10.1088/0964-1726/24/4/045018.

[16] R. Darleux, B. Lossouarn, I. Giorgio, F. dell'Isola, and J.-F. Deü, "Electrical analogs of curved beams and application to piezoelectric network damping," *Mathematics and Mechanics of Solids*, vol. 27, no. 4, pp. 578–601, 2022. DOI: 10.1177/10812865211027622. eprint: https://doi.org/10.1177/10812865211027622. [Online]. Available: https://doi.org/10.1177/10812865211027622.

[17] P. Chidamparam and A. W. Leissa, "Vibrations of Planar Curved Beams, Rings, and Arches," *Applied Mechanics Reviews*, vol. 46, no. 9, pp. 467–483, Sep. 1993, ISSN: 0003-6900. DOI: 10.1115/1.3120374. eprint: https://asmedigitalcollection.asme.org/appliedmechanicsreviews/article-pdf/46/9/467/5436807/467_1.pdf. [Online]. Available: https://doi.org/10.1115/1.3120374.

[18] T. Lang, "Vibration of thin circular rings," *Jet Propulsion Laboratory, California Institute of Technology*, 1962.

[19] L. Pernod, B. Lossouarn, J. A. Astolfi, and J. F. Deü, "Vibration damping of marine lifting surfaces with resonant piezoelectric shunts," *Journal of Sound and Vibration*, vol. 496, p. 115 921, Mar. 2021. DOI: 10.1016/j.jsv.2020.115921. [Online]. Available: https://hal.archives-ouvertes.fr/hal-03106873.

[20] B. Lossouarn, G. Kerschen, and J. Deü, "An analogue twin for piezoelectric vibration damping of multiple nonlinear resonances," *Journal of Sound and Vibration*, vol. 511, p. 116 323, 2021, ISSN: 0022-460X. DOI: https://doi.org/10.1016/j.jsv.2021.116323. [Online]. Available: https://www.sciencedirect.com/science/article/pii/S0022460X21003825.